International Journal of GEOMATE, Sept. 2022, Vol.23, Issue 97, pp.203-210
ISSN: 2186-2982 (P), 2186-2990 (O), Japan, DOI: https://doi.org/10.21660/2022.97.7554
Geotechnique, Construction Materials, and Environment

CHARACTERIZATION OF PHYSICALLY AND CHEMICALLY ACTIVATED CARBON DERIVED FROM PALM KERNEL SHELLS

Hisbullah[1], Siti Kana[1], Nabila[1] and Muhammad Faisal[1,2*]

[1]Department of Chemical Engineering, Universitas Syiah Kuala, Banda Aceh, Indonesia
[2]Halal Research Center, Universitas Syiah Kuala, Banda Aceh, Indonesia

*Corresponding Author, Received: 1 Oct. 2021, Revised: 20 June 2022, Accepted: 03 July 2022

ABSTRACT: This research aimed to characterize the physically and chemically activated carbons derived from charred palm kernel shells pyrolyzed at 400°C for 3 h in a slow pyrolysis batch reactor. The pyrolysis products were liquid smoke, charcoal, and tar. For the physical activation, the charcoal was carbonized at 600°C for 3 h in a furnace. For the chemical activation, 0.1 M NaOH, 0.1 M HCl, and 3% liquid smoke were used as activators (impregnation time: 24 h). The activated carbons were subsequently characterized by Fourier transform infrared (FTIR), scanning electron microscopy (SEM), and X-ray diffraction (XRD) analyses. The results indicated that the activated carbons met the Indonesian Industry Standard No. 0258-88. The chemical pore size: 287.9 nm–3.965 μm). The XRD analysis showed a broad peak at 2θ = 22.76°, indicating the formation of a SiO_2 amorphous structure. The FTIR analysis results indicated that the absorption patterns of the activated carbons demonstrated the presence of the functional groups O–H, C=O, C–H, and C=C; the presence of O–H and C–O indicated that the activated carbons were polar. The NaOH-activated carbon was then used to adsorb cadmium ions in a semi-continuously packed bed column, and it demonstrated a removal efficiency of 38%.

Keywords: Activated Carbon, Palm Kernel Shells, Activation, SEM, XRD, FTIR

1. INTRODUCTION

Activated carbon is a microcrystalline adsorbent with a pore structure so designed to increase its internal porosity. Activated carbons exhibit high porosity, large surface area, high surface reactivity, and high specific surface area, which all affect their adsorption capability.

Activated carbon can be produced from various materials. Generally, these materials are fossil-based hydrocarbons (e.g., coal and lignite), natural biomass (lignocellulosic materials), biomass wastes, polymers, and carbon wastes [1]. The biomass that is commonly used as a source of activated carbon includes corn cobs [2], wheat straw [3], zeolites [4], bagasse [5], tea factory waste, almond shells, tomato stems, and leaves [1], Moringa oleifera [6], oyster shells [7], coconut shells [8], coconut husks [9], and pistachio shells [10]. Natural biomass is commonly utilized to produce activated carbon not only because they are the most abundant renewable raw material but also because they are cheap and easy to obtain.

Palm kernel shells obtained from oil palm trees (Elaeis guineensis) have been widely used to produce activated carbon; palm kernel shells contain lignocellulose, making them an excellent raw material, and they are a good precursor of high-quality activated carbon [11]. The characteristics of activated carbon are strongly influenced by the composition of the parent material, the activation method employed (physical or chemical activation), the activating agent used, and the t treatment process.

Activated carbon derived from palm kernel shells can be prepared through pyrolysis, with the resulting charcoal being activated either physically or chemically. Pyrolysis is an important technology in all biomass utilization processes, in which biomass is heated to obtain such products as gas, liquid smoke, tar, and charcoal. Liquid smoke from biomass pyrolysis has been used in various applications. However, charcoal, which is a pyrolysis residue that is massively produced, has not been fully utilized. Once the charcoal is turned into activated carbon, it becomes a high-value-added product.

Generally, carbon is activated via physical, chemical, and physicochemical means. Studies have found that chemical activation is more favorable than physical activation in terms of the resulting pore structure, which determines the adsorption capability of activated carbon. Thus, chemical activation is one of the most widely used activation methods. Sodium hydroxide (NaOH), zinc chloride, potassium hydroxide, and phosphoric acid are chemical reagents often used in carbon activation processes. Activation is expected to improve the properties of charcoal, which consequently demonstrate increased adsorption capability. However, carbon derived from palm kernel shells and activated via various methods

heaviest yet to be characterized. Thus, this study aims to characterize the active carbon obtained from palm kernkernelspared through physical activation (heating at 600°C) and chemical activation (with NaOH, hydrochloric acid (HCl), and liquid smoke as activators).

2. METHODOLOGY

Palm kernel shells were pyrolyzed in a pyrolysis reactor at 400°C. The charcoal produced was crushed using a ball mill and then passed through a sieve with 80–100 mesh size. The charcoal preparation process has been detailed by Faisal et al. [12].

The activation process was carried out as follows: For the physical activation, the charcoal was heated at 600°C in a furnace (Muffle Furnace Nabertherm, LV/T/3/HA) for 3 h. For the chemical activation, 0.1 M NaOH, 0.1 M HCl, and 3% liquid smoke were used as activators, into which the charcoal was immersed for 24 h. The activated carbon was filtered and washed in distilled water until it had neutral pH and was dried at 105°C in an oven dryer (MEMMERT Drying Oven, GE-171 32 L)) for 1 h.

The resulting activated carbons were characterized by scanning electron microscopy (SEM) (Carl Zeiss Evo MA 10 Netherlands), X-ray diffraction (XRD) (XRD-7000, Shimadzu), and Fourier transform infrared (FTIR) (IR Prestige 21, Shimadzu).

Preliminary experiments were subsequently conducted, wherein the NaOH-activated carbon (AN) was used to adsorb cadmium (Cd) ions in semi-continuously packed bed columns (inside diameter: 21 mm; bed height: 35 cm). All experiments were carried out at room temperature. The initial metal concentrations were 30, 60, 90, 120, and 150 mg/L. The Cd(II) concentration was analyzed with an atomic absorption spectrophotometer (AA-7000, Shimadzu, Japan).

3. RESULTS AND DISCUSSION

3.1 Moisture and Ash Contents

Table 1 shows that each sample had a relatively low moisture content of 4%–6.5%, which met the quality standard for activated carbon as required by the Indonesian Industry Standard (IIS) No. 0258-88; the IIS has set the maximum allowable moisture content to 10%. This result is consistent with the findings of Harahap et al. [13], who reported a moisture content of 4.5%–10%.

The analysis results showed that the HCl-activated carbon (AH), the AN, the liquid smoke-activated carbon (AA), and the non-activated carbon (NA) had ash contents of 6.8%, 7%, 8.8%, and 9.7%, respectively, which met the standard. The physically activated carbon with the use of a furnace (AF) had the highest ash content at 14%, which was probably caused by the heating at 600°C. A high ash content indicates a high amount of organic matter, and it reduces the ability of carbon to remove gas or liquid [14]. Meanwhile, AH had the lowest ash content (6.8%), as HCl dissolves minerals by degrading cellulose in carbon [15].

3.2 Compound and Size Characterizations via XRD Analysis

An XRD analysis was carried out to determine the composition and crystallinity of the activated carbon as indicated by peaks at 2θ. The XRD patterns are presented in Fig. 1.

Table 1 Moisture and ash contents of the activated carbons

Parameter	Quality Standard (SII No. 0258-88)	Adsorbent	Analysis Results (%)
Moisture content	Max. 10%	NA	6.5
		AN	4.7
		AH	5.2
		AA	5.8
		AF	4.0
Ash content	Max. 10%	NA	9.7
		AN	7
		AH	6.8
		AA	8.8
		AF	14.0

Note: The carbons produced in this study were the non-activated carbon (NA), the NaOH-activated carbon (AN), the HCl-activated carbon (AH), and the liquid smoke-activated carbon (AA), and the physically activated carbon with the use of a furnace (AF).

Figure 1 shows the XRD data obtained at 2θ indicating the presence of SiO_2 in each sample, as follows: AF: 12.28° and 18.74°; AA: 20.28° and 21.43°; AH: 26.71° and 20.92°; and AN: 22.76° and 20.76° for SiO_2 and 25.60° for Al_2O_3. The SiO_2 contents of the activated carbons are presented in Table 2.

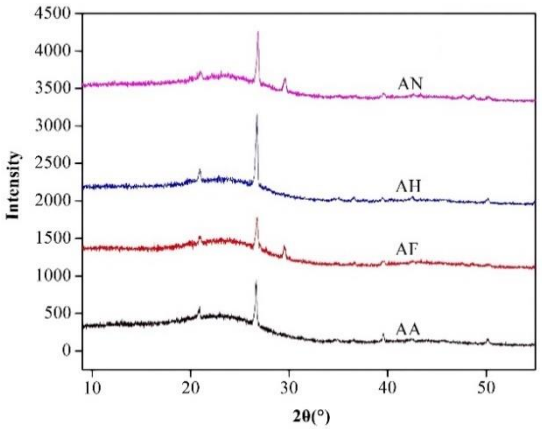

Fig. 1 XRD patterns for AN, AH, AF, and AA

Table 2. SiO_2 contents of the activated carbons derived from pyrolyzed palm kernel shells

Activated carbon	SiO_2 composition (%)
AN	93.8
AH	81.0
AA	79.4
AF	76.2

Figure 2 shows the crystallinity of the activated carbon derived from pyrolyzed palm shells and subjected to various activation methods; crystallinity was calculated using the Scherrer equation [16]. The crystallinity of AH, AF, AA, and AN (activated carbons) were 30.51, 7.18, 1.64, and 1.55 nm, respectively. AN had a lower crystallinity, and the presence of amorphous SiO_2 is visible in its XRD spectrum at 2θ = 20.76°. This result confirms the findings of Simatupang and Devi [17], wherein the silica with a peak that widened at around 2θ = 20°–22° indicated the presence of an amorphous structure (low crystallinity).

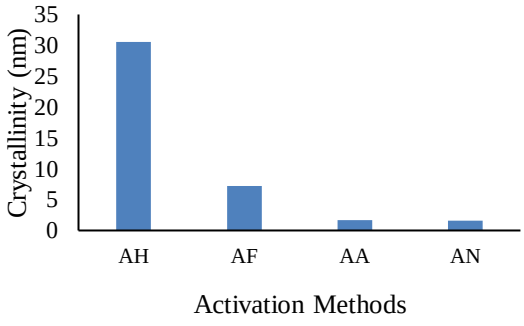

Fig. 2 Crystallinity of the activated carbons prepared using various activation methods

In addition, AN showed a 2θ shift, which caused a slight irregular sharp peak for the observed crystalline structure. This phenomenon was observed because the NaOH activation altered the palm shell crystals. The characteristics of the amorphous silica are indicated by the sloping peaks at 2θ = 22° [18].

3.3 Structural and Morphological Analyses involving SEM

The surface morphology of the activated carbons was examined at 5,000× magnification, and the results are presented in Fig. 3. The SEM analysis results showed that AH, AA and AF had particle sizes of 389.6 nm–1.329 μm, 481.2 nm–985.4 nm, and 733.7 nm–3.863 μm, respectively. The pores resulted from the evaporation and dissolution of the non-carbon contents of the palm shells during the pyrolysis process, leaving empty spaces that formed a porous structure [19].

The three activated carbons above displayed irregular particle shapes, and impurities covered the pore surface. This is because activated carbons easily dissolve in an acidic environment [20]; thus, activation in an acidic environment reduces the particle size of activated carbon, whereas furnace activation results in high ash content, although these impurities clog the pores of the activated carbon, reducing its surface area.

SEM analysis results for the NA (non-activated carbon) showed that the prepared carbon had a particle size below 500 nm, as well as a rough and irregular pore surface, consistent with the findings of Faisal et al. [21]. Meanwhile, AN (activated carbon) had a particle size of 287.9 nm–3.965 μm and had open pores with a cleaner surface compared with the other activated carbons. This finding is attributed to the ability of NaOH to minimize tar formation and dissolve impurities. In addition, NaOH activation reduces the number hydrocarbons, rendering the surface of the AN more visible. A good pore formation can increase the ability of activated carbons to adsorb heavy metals [22]. The above finding is in line with that reported by Faisal et al. [21,23], who found that the particles of a liquid smoke-activated carbon are smaller (<500 nm) than those of the carbon activated with NaOH under the same conditions and using the same activation method (immersion in a solution for 24 h).

3.4 Functional Group Analysis using FTIR

The chemical functional groups of NA, AN, and AA, which were used as adsorbents, were identified using FTIR at a frequency range of 500–4000 cm−1.

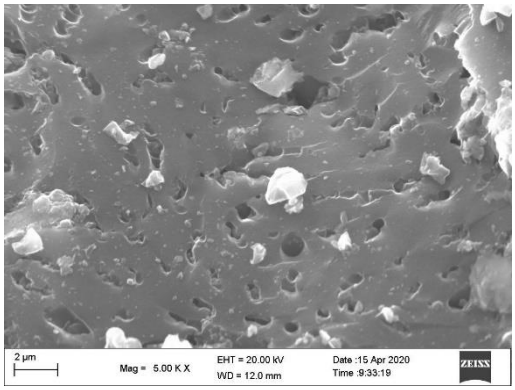

(a) AH

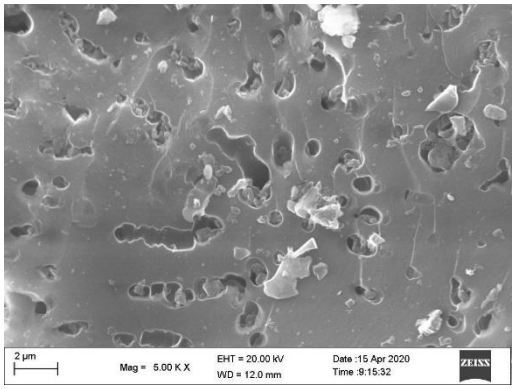

(b) AA

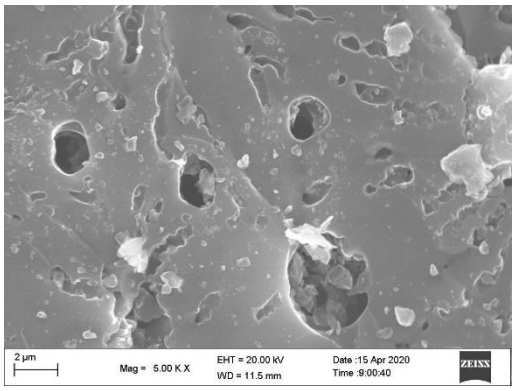

(c) AN

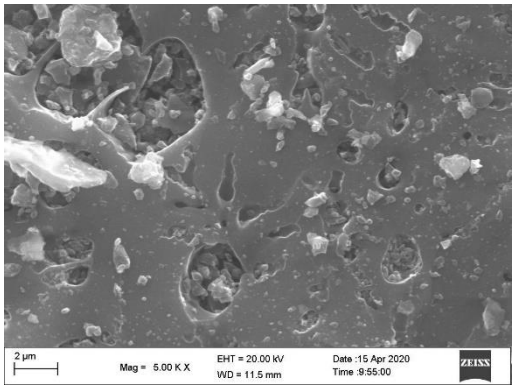

(d) AF

Fig. 3 SEM analysis results for the carbons derived from palm kernel shell and subjected to various activation methods. The SEM analysis was performed at 5,000× magnification.

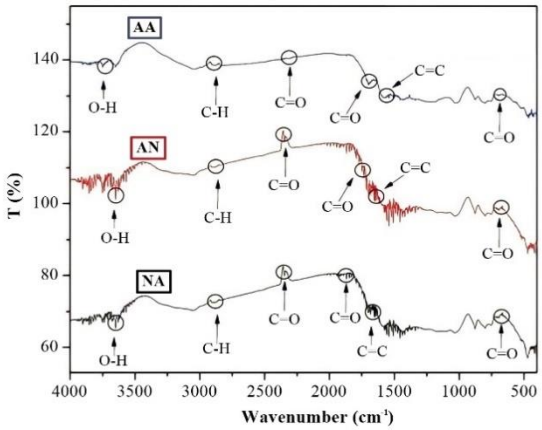

Fig. 4 FTIR analysis results for NA, AN, and AA

Figure 4 shows that in NA, peaks indicating the presence of aldehyde, ketone, and carboxylate groups were observed at 1791.87 cm−1. In AN, the intensities of the peaks corresponding to these groups decreased, whereas their intensities in AA increased. This is because NaOH is alkaline, whereas liquid smoke is acidic, resulting in a decrease in adsorption peak, an indication of the formation of aromatic compounds [24]. The adsorption intensity observed within the wavelength region resulted in a structural change in the functional group.

The FTIR analysis results for AH, AN, and AA showed that the absorption of the functional groups O–H, C–H, C=O, and C=C dominated in these three activated carbons. The presence of O–H and C–O bonds indicated that the activated carbons produced were polar. The O–H functional group bears a negative charge, which is highly reactive to metals, whereas the C=O group is typically found in activated carbons and increases their adsorption performance [19]. This confirms the findings of Razi et al. [25], who found that the presence of the O–H group as the main functional group in NaOH-activated carbon derived from palm shells contributes to the removal of pollutants from water. Table 3 presents the FTIR spectra of NA, AN, and AA.

3.5 Effects of Initial Concentration on Adsorption Capacity and Removal Efficiency of Cd(II)

The Cd adsorption performance of the NaOH-activated adsorbent during a semi-continuous operation involving various initial concentrations is presented in Fig. 5.

Table 3. FTIR spectra of the carbons derived from pyrolyzed palm kernel shells

Functional group	Bonds	Reference	Wavenum-ber (cm^{-1})
			Before activated
Hydroxyl	O-H	4000-3400	3743.83
Aromatic Alkyls	C-H	3000-2700	2837.29
Aldehydes, Ketones, Carboxyl Acids	C=O	1900-1650	1791.87
Aromatic Alkenyl	C=C	1690-1450	1543.05
			NaOH activated
Hydroxyl	O-H	4000-3400	3751.55
Aromatic Alkyls	C-H	3000-2700	2839.22
Aldehydes, Ketones, Carboxyl Acids	C=O	1900-1650	1766.80
Aromatic Alkenyl	C=C	1690-1450	1560.41
			Liquid smoke activated
Hydroxyl	O-H	4000-3400	3745.76
Aromatic Alkyls	C-H	3000-2700	2879.72
			Liquid smoke activated
Aldehydes, Ketones, Carboxyl Acids	C=O	1900-1650	1915.31
Aromatic Alkenyl	C=C	1690-1450	1575.84

Figure 5 shows that at the initial concentration of 120 mg/L and adsorption time of 4 h, the adsorbent demonstrated the highest adsorption capacity of 0.007942 mg/g. This result showed that the adsorption capacity increased with the increase in initial Cd(II) concentration, as the active sites became occupied more easily. The adsorbate ion saturated the adsorbent more easily and reached equilibrium more quickly with the increase in initial influent concentration due to a larger driving force for mass transfer, allowing the transfer process to overcome the mass transfer barriers in the column [26].

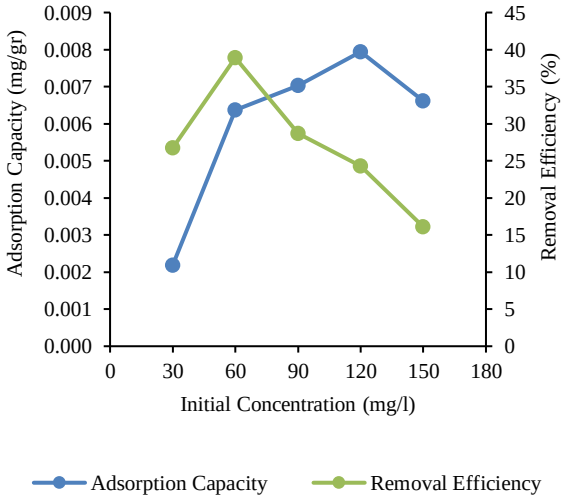

Fig. 5. Effects of initial concentrations on adsorption capacity and removal efficiency of Cd(II) (pH 5, flow rate 10 mL/min)

The higher the concentration, the higher the adsorption capacity. However, at 150 mg/L, the adsorption capacity decreased. This observation can be explained by the larger concentration gradient causing faster transport due to an increase in diffusion coefficient or mass transfer coefficient. The high initial solution concentration provided a higher driving force that allows the transfer process to overcome the mass transfer barriers [27].

The above finding is consistent with that reported by Garba et al. [28], who found that the highest adsorption capacity was achieved at the initial solution concentration of 120 mg/L, which was then considered the optimum condition for an adsorption process. However, the metal removal efficiency was inversely proportional to the adsorption capacity. Baby and Hussein [29], who investigated heavy metal adsorption using activated carbon derived from oil palm shells, showed that metal removal efficiency decreased with increasing metal ion concentration due to saturation at the adsorbent site. The initial solution concentrations of 30, 60, and 90 mg/L showed a good efficiency at 26.72%, 38.9%, and 37.31%, respectively. At the higher concentrations of 120 and 150 mg/L, the adsorption efficiency decreased to 24.27% and 16.16%, respectively.

3.6 Effects of pH on Adsorption Capacity and Removal Efficiency of Cd(II)

pH is one of the important parameters influencing adsorption capacity, as it affects the adsorbent surface and is related to protonation or deprotonation on the activated side of the adsorbent surface. It can also affect the chemical balance of both the adsorbate and the adsorbent [30]. The effects of pH on Cd adsorption are presented in Fig. 6.

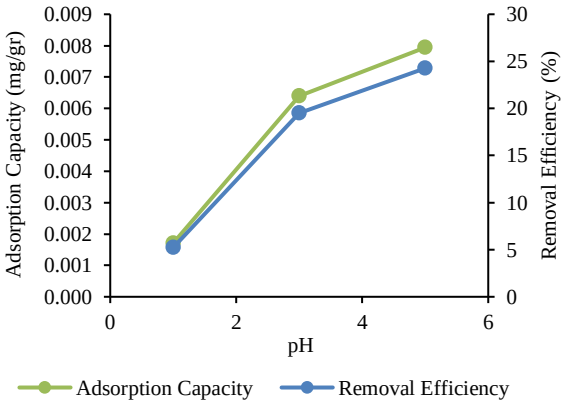

Fig. 6. Effects of pH on the adsorption capacity and removal efficiency of Cd(II) (initial concentration: 120 mg/L; flow rate: 10 mL/min)

Fig. 6 shows that the adsorption capacity increased with increasing pH. This is because the active groups on the adsorbent surface were filled with adsorbate, so the chance for bonding between Cd and the active site of the adsorbent decreased [31]. In addition, the metal adsorption efficiency increased significantly when the pH was increased from 1 to 5. At pH 1, 3, and 5, the removal efficiencies were 5.23%, 19.52%, and 24.27%, respectively. The association of metal ions with the adsorbent surface was strongly influenced by the pH of the solution, where the maximum metal ion removal occurred at an acidic pH. A further increase above the optimum pH caused the formation of metal ion deposits, while at a lower pH, the adsorbent was protonated, and the protons competed with the metal ions, resulting in reduced adsorption [32].

At pH 1, the adsorption capacity was at its lowest at 0.001711 mg/g. This was because, at an acidic pH, ions tend to dissolve, reducing the ability of the adsorbent's active group to bind metal ions. In addition, at an acidic pH, the adsorbent surface was surrounded by H+ ions, rendering it positively charged. This resulted in repulsion between the adsorbent surface and the metal ions, resulting in a low adsorption capacity [30]. The maximum Cd adsorption by an activated carbon takes place at pH 4–6 [33,34].

4. CONCLUSION

The results showed that the activation method influenced the characteristics of the activated carbons derived from palm kernel shells. The NaOH-activated carbon had a moisture content of 4.7% and an ash content of 7%, and it was the best-activated carbon based on the SII standard. This activated carbon displayed a clean and even surface and had a crystalline value of 1.55 nm, indicating the presence of amorphous SiO_2; moreover, its SiO_2 content was 93.8%. The FTIR analysis showed that the adsorption in all of the activated carbons was dominated by O–H, C–H, C=O, and C=C groups and that the activated carbons were polar. Preliminary results showed that the NaOH-activated carbon could adsorb Cd(II), with a removal efficiency of 38%. These results suggested that further research is needed to evaluate the performance of each activated carbon for the adsorption of various chemical compounds, especially those found in industrial wastes.

5. ACKNOWLEDGMENTS

The authors would like to acknowledge the funding support and the research facilities provided by the Universitas Syiah Kuala and the Ministry of Education, Culture, Research and Technology of the Republic of Indonesia

6. REFERENCES

[1] Tiryaki B., Yagmur E., Banford A., and Aktas Z., Comparison of Activated Carbon Produced from Natural Biomass and Equivalent Chemical Compositions. Journal of Analytical and Applied Pyrolysis, Vol. 105, 2014, pp. 276-283.

[2] Feng P., Li J., Wang H., and Xu Z., Biomass-based Activated Carbon and Activators: Preparation of Activated Carbon from Corncob by Chemical Activation with Biomass Pyrolysis Liquids. ACS Omega, Vol. 5, Issue 37, 2020, pp. 24064-24072.

[3] Naeem M.A., Imran M., Amjad M., Abbas G., Tahir M., Murtaza B., Zakir A., Shahid M., Bulgariu L., and Ahmad I., Batch and Column Scale Removal of Cadmium from Water Using Raw and Acid Activated Wheat Straw Biochar. Journal of Water, Vol.11, Issue 7, 2019, pp. 1-17.

[4] Barragan-Pena P., Marcedo-Miranda M.G., and Olguin M.T., Cadmium Removal from Wastewater in a Fixed-Bed Column System with Modified-Natural Clinoptilolite-Rich Tuff. Chemical Papers, Vol. 75, 2020, pp. 485-491.

[5] Xavier A.L.P., Adarme O.F.H., Furtado L.M., Ferreira G.M.D., Silva L.H.M., Gil L.F., and Gurgel L.V.A., Modelling Adsorption of Copper (II), Cobalt (II) And Nickel (II) Metal Ions from Aqueous Solution onto a New Carboxylated Sugarcane Bagasse. Part II: Optimization of Monocomponent Fixed-Bed Column Adsorption. Journal of Colloid and Interface Science, Vol. 516, 2018, pp. 431-445.

[6] Rajeshwari M., Agrawal P., Pavithra S., Priya, Sandhya G.R., and Pavithra, G.M., Continuous Biosorption of Cadmium by *Moringa olefera* in a Packed Column. Biotechnology and Bioprocess Engineering, Vol. 18, Issue 2, 2013, pp. 321–325.

[7] Yan-jiao G., Cadmium and Cobalt Removal from Heavy Metal Solution Using Oyster Shells Adsorbent. Asian Journal of Chemistry, Vol. 25, Issue 15, 2011, 1098-1101.

[8] Sousa F.W., Oliveira A.G., Ribeiro J.P., Rosa M.F., Keukeleire D., Nascimento R.F., Green Coconut Shells Applied as Adsorbent for Removal of Toxic Metal Ions Using Fixed-Bed Column Technology. Journal of Environmental Management, Vol. 91, Issue 8, 2010, pp. 1634-1640.

[9] Amarasinghe, B.M.W.P.K., Lead and Cadmium Removal from Aqueous Medium Using Coir Pith as Adsorbent: Batch and Fixed Bed Column Studies. Journal of Tropical Forestry and Environment, Vol. 1, Issue 1, 2011, pp. 36-47.

[10] Banerjee M., Bar N., Basu R.K., and Das R.K., Removal of Cr(VI) from Its Aqueous Solution Using Green Adsorbent Pistachio Shell: A Fixed Bed Column Study and GA-ANN Modeling. Water Conservation Science and Engineering, Vol. 3, Issue 1, 2018, pp. 19-31.

[11] Faisal M., Abubakar, Kelana S.P, and Nanda D.E., Removal of Cu^{2+} Ions Using Activated Carbon from Palm Kernel Shell Waste by Liquid Smoke Activation. International Journal on Advanced Science Engineering Information Technology, Vol. 10, Issue 6, 2020, pp. 2560-2566.

[12] Faisal M., Gani A., Husni, and Daimon H., A Preliminary Study of the Utilization of Liquid Smoke from Palm Kernel Shells for Organic Mouthwash. International Journal of GEOMATE, Vol. 13, Issue 37, 2017, pp. 116-120.

[13] Harahap H.H., Malik U., and Dewi R., Pembuatan Karbon Aktif dari Cangkang Kelapa Sawit dengan Menggunakan H_2O sebagai Aktivator untuk Menganalisis Proksimat, Bilangan Iodine dan Rendemen. Jurnal Online Mahasiswa Universitas Riau, Vol. 1, Issue 2, 2014, pp. 48-54.

[14] Laos L. E., and Selan A., Pemanfaatan Kulit Singkong sebagai Bahan Baku Karbon Aktif. Jurnal Ilmu Pendidikan Fisika, Vol. 1, Issue 1, 2016, pp. 32-36.

[15] Setiyoningsih L.A., Dwi I., and Tri M., Pembuatan dan Karakterisasi Arang Aktif Kulit Singkong Menggunakan Aktivator $ZnCl_2$. Jurnal Kimia Riset, Vol. 3, Issue 1, 2018, pp. 13-19.

[16] Silas K., Ghani W.A.W.A.K., Choong T.S.Y., and Rashid U., Activated Carbon Monolith CO_3O_4 Based Catalyst: Synthesis, Characterization and Adsorption Studies. Environmental Technology and Innovation, Vol. 12, Issue 4, 2018, pp. 273-285.

[17] Simatupang L., and Devi, The Preparation and Characterization of Sinabung Volcanic Ash as Silica Based Adsorbent. Jurnal Pendidikan Kimia, Vol. 8, Issue 3, 2016, pp. 159-163.

[18] Su Y., Liu L., Zhang S., Xu D., Du H., Cheng Y., Wang Z., and Xiong Y., A Green Route for Pyrolysis Poly-Generation of Typical High Ash Biomass, Rice Husk: Effects on Simultaneous Production of Carbonic Oxide-Rich Syngas, Phenol-Abundant Bio-Oil, High-Adsorption Porous Carbon and Amorphous Silicon Dioxide. Bioresource Technology, Vol. 295, 2019, pp. 122243.

[19] Mentari V.A., Handika G., and Maulina S., Perbandingan Gugus Fungsi dan Morfologi Permukaan Karbon Aktif dari Pelepah Kelapa Sawit Menggunakan Aktivator Asam Fosfat (H_3PO_4) dan Asam Nitrat (HNO_3). Jurnal Teknik Kimia USU, Vol. 7, Issue 1, 2018, pp. 16–20.

[20] Wu Z.C., Wang Z.Z., Liu J., Yin J.H., and Kuang S.P., A New Porous Magnetic Chitosan Modified by Melamine for Fast and Efficient Adsorption of Cu(II) Ions. International Journal of Biological Macromolecules, Vol.81, 2015, pp. 838-846.

[21] Faisal M., Gani A., and Fuadi Z., Utilization of Activated Carbon from Palm Kernel Shells as the Bioadsorbent of Lead Waste. International Journal of GEOMATE, Vol. 20, Issue 78, 2021, pp. 81-86.

[22] Verayana, Paputungan M., and Iyabu H. Pengaruh Aktivator HCl dan H_3PO_4 Terhadap Karakteristik (Morfologi Pori) Arang Aktif Tempurung Kelapa Serta Uji Adsorpsi Pada Logam Timbal (Pb). Jambura Journal of Educational Chemistry, Vol. 13, Issue 1, 2018, pp. 67-75.

[23] Faisal M., Gani A., and Abubakar, Removal of Copper Ions from Aqueous Solution Using Palm Shell Charcoal Activated by NaOH. International Journal of GEOMATE, Vol. 15, Issue 48, 2018, pp. 143-147.

[24] Mohideen M.F, Faiz M., Salleh H., Zakaria H., and Raghavan V., Drying of Oil Palm Frond

Via Swirling Fluidization Technique. In Proceedings of the World Congress on Engineering, Vol. 3, 2011, pp. 2375-2380.

[25] Razi M.A.M, Al-Gheeti A., Al-Qaini M., and Yousef, A., Efficiency of Activated Carbon from Palm Kernel Shell for Treatment of Greywater. Arab Journal of Basic and Applied Sciences, Vol. 25, Issue 3, 2018, pp. 103–110.

[26] Bakar, A.H.A., Abdullah, L.C., Zahri, N.M.M., and Alkhatib, M., Column efficiency of fluoride removal using quaternized palm kernel shell (QPKS). International Journal of Chemical Engineering, 2019, pp. 1-13.

[27] Chen, S., Yue, Q., Gao, B., Li, Q., Xu, X., and Fu, K., Adsorption of Hexalent Chromium from Aqueous Solution by Modified Corn Stalk: A Fixed-Bed Column Study. Bioresource Technology, 2012, pp. 114-120.

[28] Garba, Z.N., Ugbaga, N.I., and Abdullahi, A.K., Evaluation of Optimum Adsorption Conditions for Ni (II) and Cd (II) Removal from Aqueous Solution by Modified Plantain Peels (MPP). Beni-Suef University Journal of Basic and Applied Sciences, Vol. 5, Issue 2, 2016, pp.170-179.

[29] Baby, R., and Hussein, M.Z., Ecofriendly Approach for Treatment of Heavy-Metal-Contaminated Water using Activated Carbon of Kernel Shell of Oil Palm. Materials, Vol. 13, Issue 11, 2020, pp. 1-14.

[30] Adam, D.N., Suyani, H., Nasir, M., Safni., and Nugraha, W.C., Adsorpsi Cu Menggunakan Nanofiber Polisulfon-FeOOH yang Disintesis dengan Metode Electrospinning. Jurnal Litbang Industri, Vol. 3, Issue 2, 2013, pp. 101-108.

[31] Darjito, Purwonugroho, D., and Nisa, S.N., Study on Adsorption of Cd(II) by Chitosan-Alumina. Journal of Chemistry, Vol. 6, Issue 3, 2006, pp. 238-244.

[32] Mustapha, S., Shuaib, D.T., Ndamitso, M.M., Etsuyankpa, M.B., Sumaila, A., and Mohammed, U.M., Adsorption Isotherm, Kinetic and Thermodynamic Studies for the Removal of Pb(II), Cd(II), Zn(II) and Cu(II) Ions from Aqueous Solutions using Albizia Lebbeck Pods. Applied Water Science, Vol. 9, Issue 142, 2019, pp. 1-11.

[33] Machida, M., Fotoohi, B., Amano, Y. Ohba, T., Kanoh, H., and Mercier, I., Cadmium (II) Adsorption using Functional Mesoporous Silica and Activated Carbon. Journal of Hazard Materials, 2012, pp. 220-227.

[34] Naeem, M. A., Imran, M., Amjad, M., Abbas, G., Tahir, M., Murtaza, B., Zakir, A., Shahid, M., Bulgariu, L., and Ahmad, I., Batch and Column Scale Removal of Cadmium from Water using Raw and Acid Activated Wheat Straw Biochar. Journal of Water, Vol. 11, Issue 7, 2019, pp. 1-17.

Copyright © Int. J. of GEOMATE All rights reserved, including making copies unless permission is obtained from the copyright proprietors.